Available online at www.sciencedirect.com
ScienceDirect
C. R. Acad. Sci. Paris, Ser. I 343 (2006) 431–436
COMPTES RENDUS MATHEMATIQUE
http://france.elsevier.com/direct/CRASS1/

Numerical Analysis

Computation of the normal vector to a free surface by a finite element – finite volume mixed method

Alexandre Caboussat [a], Roland Glowinski [a,b], James M. Sicilian [c]

[a] *Department of Mathematics, University of Houston, Houston, TX 77204-3008, USA*
[b] *Laboratoire J.L. Lions, Université P. et M. Curie, 4, place Jussieu, 75005 Paris, France*
[c] *CCS-2, Methods for Adv. Sci. Simulations, Los Alamos National Laboratory, Los Alamos, NM 87545, USA*

Received 19 July 2006; accepted 26 August 2006

Presented by Philippe G. Ciarlet

Abstract

In volume tracking finite volume schemes for free surface flows, the reconstruction of the interface and the computation of surface tension effects require an accurate approximation of the normal vector to the interface. A numerical method for the computation of the normal vector is presented here, based on a finite element approach. We use projections to interpolate the volume fraction of liquid between the finite volume mesh and a nested finite element mesh. Error estimates are obtained and numerical results show the efficiency and flexibility of the approach discussed here. ***To cite this article: A. Caboussat et al., C. R. Acad. Sci. Paris, Ser. I 343 (2006).***

Résumé

Calcul du vecteur normal à une surface libre par une méthode mixte d'éléments finis – volumes finis. Dans la plupart des schémas de type volume finis pour des problèmes de surface libre, la reconstruction de l'interface et le calcul des effets de tension de surface nécessitent une approximation précise du vecteur normal à l'interface. Nous présentons une méthode numérique pour le calcul du vecteur normal, basée sur une approche de type éléments finis. Nous interpolons la fraction liquide de la grille volumes finis sur un maillage emboité de type éléments finis à l'aide de projections. Nous obtenons des estimations d'erreurs a priori et l'efficacité de la méthode est confirmée par les résultats d'essais numériques. ***Pour citer cet article : A. Caboussat et al., C. R. Acad. Sci. Paris, Ser. I 343 (2006).***

1. Introduction

In free surface flow simulations, the accurate approximation of the free surface between two media is a crucial issue. In finite volume based volume tracking methods, the reconstruction of the interface between two or more media is required. Several models for the reconstruction of the interface exist in the literature. For instance the PLIC (*Piecewise linear interface calculation*) procedure [1,11] requires an approximation of the normal vector to the free

E-mail addresses: caboussat@math.uh.edu (A. Caboussat), roland@math.uh.edu (R. Glowinski), sicilian@lanl.gov (J.M. Sicilian).

1631-073X/$ – see front matter
doi:10.1016/j.crma.2006.08.010

surface in each interface cell of the discretization to determine the orientation of the interface [6]. An approximation of the normal vector is also needed for the computation of the surface tension effects [7] and the fluxes [9]. We present a consistent approximation of the normal vector in each cell of a finite volume mesh composed by hexahedra, based on an auxiliary nested finite element mesh of tetrahedra. Following the idea of [3], projections are used to obtain a piecewise linear finite element approximation of each volume fraction on the finite element mesh [2]. The values of the normal vector are obtained by Clément interpolation [4] at the vertices of the finite element mesh. Error estimates are obtained to highlight the effect of the additional procedure on the total error of the scheme.

2. The model and a finite volume scheme

Let Ω be a bounded domain in two or three space dimensions and $\partial\Omega$ be its boundary. Let $T > 0$ be a finite time. Let M be the total number of materials (phases) existing in the system. Let ρ denote the density of the fluid and μ its viscosity, both being constant in each material but discontinuous across the interfaces. The velocity of the fluid $\mathbf{u}$ and the pressure p are assumed to satisfy the incompressible Navier–Stokes equations, which consist of the conservation of mass and momentum in the space-time domain $\Omega \times (0, T)$:

$$\begin{aligned} &\frac{\partial(\rho\mathbf{u})}{\partial t} + \nabla\cdot(\rho\mathbf{u}\mathbf{u}) = -\nabla p + \nabla\cdot\left(\mu\left(\nabla\mathbf{u} + \nabla\mathbf{u}^{\mathrm{T}}\right)\right) + \mathbf{f}, && \text{in } \Omega\times(0,T),\\ &\nabla\cdot\mathbf{u} = 0, && \text{in } \Omega\times(0,T), \end{aligned}$$

where $\mathbf{f}$ denotes the surface and body forces applied onto the fluid. Initial conditions are imposed on the velocity $\mathbf{u}$ at time $t = 0$. Boundary conditions are classical boundary conditions on $\partial\Omega$ for the velocity $\mathbf{u}$ (slip and/or no-slip). The boundary condition at the free surface between two materials is a normal force balance given by $[-p\mathbf{n} + \mu(\nabla\mathbf{u} + \nabla\mathbf{u}^{\mathrm{T}})\cdot\mathbf{n}] = \sigma\kappa\mathbf{n}$, where $[\cdot]$ denotes the jump over the interface between the two materials, σ is the surface tension coefficient, κ is the curvature of the interface and $\mathbf{n}$ is the normal vector to the interface. The volume fraction of material k, denoted by f_k, $k = 1,\ldots,M$, is the characteristic function of the domain occupied by the material k and satisfies the advection equation:

$$\frac{\partial f_k}{\partial t} + \mathbf{u}\cdot\nabla f_k = 0, \quad \text{in } \Omega\times(0,T),\ k = 1,\ldots,M. \tag{1}$$

Let Q_h denote the finite volume (unstructured) quadrangulation of Ω and denote by Q any generic hexahedron of Q_h. The numerical algorithm is based on operator splitting theory and allows to decouple the reconstruction of the interface from the other physical phenomena. Let us consider the case with two phases ($M = 2$). Eq. (1) is solved with a finite volume scheme [5,7] to obtain an approximation of f_k at time t^{n+1} that is piecewise constant in each cell. The PLIC algorithm [1,11] allows us to reconstruct a planar approximation of the interface. The approximation of the normal vector

$$\mathbf{n}_k = \frac{\nabla f_k}{|\nabla f_k|}, \quad k = 1,\ldots,M,$$

is located at the center of each cell and gives the orientation of the local interface within the cell Q for the reconstruction of the planar interface [11].

The reconstruction of the interface in the algorithm relies on the approximation of the normal vector and uniquely determines the computation of the fluxes across each face of the cell Q. The approximation of the normal vector is also required for the computation of the surface tension effects on the interface. The computation of the surface tension effects in a finite volume framework uses an approximation of the normal vector located at the center of the cell faces that are on the interface. We refer to [5,7,11] and references therein for the extensive description of the method. The determination of the normal vector at the interface plays a central role in the whole algorithm. A consistent finite elements based technique for its approximation is presented in the following.

3. A finite element approach for the computation of the normal vector

Let h denote the maximal diameter of the cells of the finite volume mesh. Let $f \in L^2(\Omega)$ be a generic volume fraction of liquid and $f_{0,h} \in \mathbb{P}_0$ its piecewise constant approximation on Q_h [1,11] obtained with a finite volume scheme, whose values are located at the center of each cell.

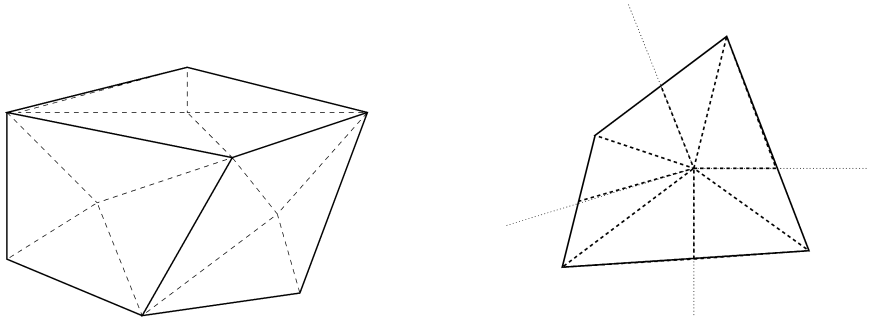

Fig. 1. Decomposition of one cell into tetrahedra. Left: one hexahedron is split into twenty-four tetrahedra in 3D. Right: one quadrangle is split into eight triangles in 2D.

A finite element mesh is nested into the initial finite volume quadrangulation as illustrated in Fig. 1. The introduction of a finite element mesh is designed in order to obtain a consistent approximation of the field f at the center of the faces of the cells and at the vertices of each cell [10]. The following decomposition is introduced. Each hexahedron is decomposed into twenty-four tetrahedra in three space dimensions, each of them with one vertex coinciding with the center of the cell, one vertex with the center of one of the faces of the cell and the remaining two vertices with two vertices of the same face. In two space dimensions, each hexahedron is similarly split in eight triangles. A similar decomposition can be made when the finite volume mesh is composed of tetrahedra.

Let us denote by $\mathcal{T}_h$ the finite element mesh described above and let K denote a generic tetrahedron of $\mathcal{T}_h$. Let N_n by the number of vertices in $\mathcal{T}_h$ and let the piecewise linear finite element basis functions based on $\mathcal{T}_h$ be denoted by φ_j, $j = 1, \ldots, N_n$. The piecewise linear approximation $f_{1,h}$ on $\mathcal{T}_h$ of f is given by the L^2-projection of $f_{0,h}$ defined by:

$$\int_\Omega f_{1,h}\varphi_j \,\mathrm{d}x = \int_\Omega f_{0,h}\varphi_j \,\mathrm{d}x, \quad \forall j = 1, \ldots, N_n. \tag{2}$$

With a mass lumping procedure, (2) is a weighted average of the adjacent values of $f_{0,h}$ for each vertex of $\mathcal{T}_h$, as in [2,3] for instance. The projection allows to obtain a piecewise linear approximation $f_{1,h}$ on the tetrahedra. The approximation $f_{1,h}$ is differentiated to obtain a piecewise constant value $\nabla f_{1,h}$ on each $K \in \mathcal{T}_h$, that is normalized to give the normal vector $\mathbf{n}_{1,h}$.

The value of the normal vector at the vertices of $\mathcal{T}_h$ is denoted by $\mathbf{n}_{0,h}$ and is given by the projection of the piecewise constant field $\mathbf{n}_{1,h}$ on the vertices of the finite element mesh:

$$\int_\Omega \mathbf{n}_{0,h}\varphi_j \,\mathrm{d}x = \int_\Omega \mathbf{n}_{1,h}\varphi_j \,\mathrm{d}x, \quad \forall j = 1, \ldots, N_n. \tag{3}$$

With a mass lumping procedure, (3) is equivalent to the Clément interpolation $r_h : H^1(\Omega) \to \mathbb{P}_1$ defined by $r_h v(P) = \frac{1}{|\Omega_P|}\int_{\Omega_P} v(x)\,\mathrm{d}x$, where P is a vertex of the finite element mesh and $\Omega_P = \bigcup\{K \in \mathcal{T}_h\colon\ P \in K\}$ [4]. Therefore $\mathbf{n}_{0,h} := r_h \mathbf{n}_{1,h}$. Consistent values of the normal vector $\mathbf{n}_{0,h}$ are thus obtained at the center of the cells of the finite volume mesh, at the center of the faces and at the vertices.

Theorem 1. *For a two-dimensional orthogonal finite volume mesh of squares, the reconstruction of the normal vector is exact when the initial volume fraction of liquid f is a bilinear function $f(x, y) = ax + by + cxy + d$, $a, b, c, d \in \mathbb{R}$.*

Proof. Without loss of generality, the parameter d can be set to zero. The piecewise constant approximation of f is initially defined as the restriction at the center of the cells. We can check that: (i) the projection of the piecewise constant approximation at the vertices of the finite element mesh is exact and the exact values of f are recovered at the vertices; (ii) the projection of the piecewise constant approximation of ∇f on the triangles at the vertices of the finite element mesh leads to the exact values of ∇f at the center of the cells, the center of the faces and the vertices of each cell. □

Error estimates justifying the use of the multi-grids method are presented in the following. Since $f \in L^2(\Omega)$, for all $\delta > 0$, there exists $f \in H^3(\Omega)$ such that

$$\|f - f_\delta\|_{L^2(\Omega)} \leqslant \delta \tag{4}$$

by density of the Sobolev spaces. Therefore error estimates can be investigated for f_δ, the purpose of the following results being only to describe the additional error introduced by the multi-grids method.

Theorem 2 *(Error estimates on the normal vector). There exists a constant C independent of h, such that*

$$\|\nabla f_\delta - r_h \nabla f_{1,h}\|_{L^2(\Omega)} \leqslant C\big\{h\|f_\delta\|_{H^2(\Omega)} + \|\nabla f_{1,h} - \nabla f_{0,h}\|_{L^2(\Omega)} + \|f_{0,h} - f_\delta\|_{H^1(\Omega)}\big\}. \tag{5}$$

The derivatives of $f_{0,h} \in \mathbb{P}_0$ in (5) are defined by a centered finite differences scheme. This result states that the error between the real derivative and the final estimate is bounded by the Clément interpolant plus the error introduced by the projection between the two grids plus the error due to the original finite volume scheme that produces $f_{0,h}$.

Proof. The triangle inequality leads to

$$\|\nabla f_\delta - r_h \nabla f_{1,h}\|_{L^2(\Omega)} \leqslant \|\nabla f_\delta - r_h \nabla f_\delta\|_{L^2(\Omega)} + \|r_h \nabla f_\delta - r_h \nabla f_{1,h}\|_{L^2(\Omega)}. \tag{6}$$

The Clément interpolant r_h is linear and bounded uniformly in h, i.e., there exists $C_r = C_r(\Omega)$ independent of h, such that, for all $v \in L^\infty(\Omega)$, $\|r_h v\|_{L^2(\Omega)} \leqslant C_r \|v\|_{L^2(\Omega)}$. Thus (6) leads to

$$\begin{aligned}\|\nabla f_\delta - r_h \nabla f_{1,h}\|_{L^2(\Omega)} &\leqslant Ch\|f_\delta\|_{H^2(\Omega)} + C_r\|\nabla f_{1,h} - \nabla f_\delta\|_{L^2(\Omega)} \\ &\leqslant Ch\|f_\delta\|_{H^2(\Omega)} + C_r\|\nabla f_{1,h} - \nabla f_{0,h}\|_{L^2(\Omega)} + C_r\|\nabla f_{0,h} - \nabla f_\delta\|_{L^2(\Omega)}\end{aligned}$$

and relation (5) holds. □

Theorem 3 *(Projection error in the two-dimensional orthogonal case). For a two-dimensional orthogonal finite volume grid (composed of squared cells) and when each cell is decomposed into eight triangles, there exists a constant C independent of h such that*:

$$\|\nabla f_{0,h} - \nabla f_{1,h}\|_{L^2(\Omega)} \leqslant Ch, \quad \forall h \leqslant 1, \tag{7}$$

where $\nabla f_{0,h} \in \mathbb{P}_0$ is defined by $\nabla f_{0,h}(P_{ij}) = \frac{1}{2h}(f_{i+1,j} - f_{i-1,j},\ f_{i,j+1} - f_{i,j-1})^{\mathrm{T}}$.

Proof. By density, we can assume that $f_\delta \in H^{3+\varepsilon}(\Omega)$, $\forall \varepsilon > 0$. The error on the total domain can be decomposed into individual errors on each cell C_{ij}. With the above definition of $\nabla f_{0,h}$, we can write:

$$\|\nabla f_{0,h} - \nabla f_{1,h}\|^2_{L^2(C_{ij})} = \sum_{K \subset C_{ij}} \|\nabla f_{0,h} - \nabla f_{1,h}\|^2_{L^2(K)}.$$

On each triangle $K \subset C_{ij}$, the difference between both gradients can be expressed explicitly with finite differences schemes. More precisely, there exists $\xi_{K,ij} \in K \subset C_{ij}$ such that

$$\|\nabla f_{0,h} - \nabla f_{1,h}\|^2_{L^2(K)} \leqslant C \int_K h^2\big(\nabla^2 f_\delta(\xi_{K,ij})\big)^2 \,\mathrm{d}x + \mathcal{O}\big(h^4\big). \tag{8}$$

Eq. (8) leads to $\|\nabla f_{0,h} - \nabla f_{1,h}\|^2_{L^2(\Omega)} \leqslant Ch^2\|f_\delta\|^2_{H^{3+\varepsilon}(\Omega)} + \mathcal{O}(h^4)$ and relation (7) holds. □

4. Numerical results

Numerical results are presented to validate the computation of the normal vector independently of other numerical approximations. The method has been implemented in the finite volume code TRUCHAS [5].

We consider first a static cylinder of liquid lying in a vacuum along the Oz axis, without any external body or surface forces. The radius of the cylinder in the (x, y)-plane is 1 m, while the height of the cylinder is 0.3 m. The finite volume quadrangulation is structured and orthogonal. Convergence results for the error $\|\nabla f_\delta - r_h \nabla f_{1,h}\|_{L^2(\Omega)}$

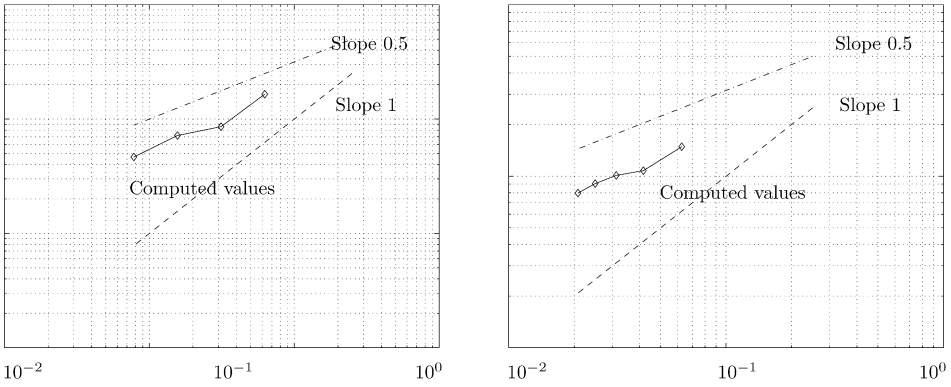

Fig. 2. Convergence orders for the error on the estimation of the normal vector. Left: the case of a static cylinder. Right: the case of a static spherical droplet.

Table 1
Comparison of absolute errors for the normal vector for the case of the static spherical droplet

h	1/8	1/16	1/32	1/48
$\|\nabla f_\delta - r_h \nabla f_{1,h}\|_{L^2(\Omega)}$ with multi-grids method	0.1484	0.1486	0.1011	0.0798
$\|\nabla f_\delta - r_h \nabla f_{1,h}\|_{L^2(\Omega)}$ with original method [11]	0.1607	0.1520	0.1025	0.0818

are based on the values of the normal vector at the center of the cells only and convergence orders are presented in Fig. 2 (left). We consider then a static spherical droplet of liquid lying in a vacuum, without gravity forces. The radius of the droplet is 1 m. When the center of the droplet is $(0, 0, 0)$, the normal vector to the liquid–void interface is given explicitly by $\mathbf{n}(x, y, z) = (x\ y\ z)^{\mathrm{T}}$. Convergence orders are presented in Fig. 2 (right).

Fig. 2 shows that, in both cases, the error on the normal vector in the total scheme is approximately of order $\mathcal{O}(h^{1/2})$ [8]. The error due to the initialization technique [5] is convergent with order 2 and therefore can be neglected. The order of magnitude of the error on the normal vector approximation with the introduction of the additional multi-grids technique is compared with the original approximation of the normal vector given by the finite volume scheme and described in [11]. Results are given in Table 1 for the case of the static spherical droplet.

We conclude that, besides a small difference in absolute errors between the two methods, the multi-grids method offers a new flexibility for the unified calculation of a consistent value of the normal vector (or other fields) not only at the center of the cells, but also at the center of the faces and at the vertices, without introducing a significant contribution to the total error of the scheme. The values of the normal vector at the center of faces and at the vertices will be useful for the estimation of surface tension effects.

Acknowledgements

The Los Alamos National Laboratory is greatly acknowledged for providing the TRUCHAS software. This work has been initiated during a visit of the first two authors in the Los Alamos National Laboratory in the summer of 2005.

References

[1] E. Aulisa, S. Manservisi, R. Scardovelli, A mixed markers and volume-of-fluid method for the reconstruction and advection of interfaces in two-phase and free-boundary flows, J. Comput. Phys. 188 (2003) 611–639.
[2] A. Caboussat, Numerical simulation of two-phase free surface flows, Arch. Comput. Methods Engrg. 12 (2) (2005) 165–210.
[3] A. Caboussat, R. Glowinski, A two-grids/projection algorithm for obstacle problems, Comput. Math. Appl. 50 (2005) 171–178.
[4] P. Clément, Approximation by finite element functions using local regularization, RAIRO Anal. Num. 9 (1975) 77–84.
[5] E.D. Dendy, J.M. Sicilian, D.B. Kothe, M. Bussmann, M.M. Francois, J. Mohd-Yusof, S.J. Cummins, Fluid flow and advection in Truchas, Technical Report LA-UR-04-4041, Los Alamos National Laboratory, 2004.
[6] R. Eymard, T. Gallouët, R. Herbin, Finite volume approximation of elliptic problems and convergence of an approximate gradient, Appl. Numer. Math. 37 (2001) 31–53.

[7] M.M. Francois, S.J. Cummins, E.D. Dendy, D.B. Kothe, J.M. Sicilian, M.W. Williams, A balanced-force algorithm for continuous and sharp interfacial surface tension models within a volume tracking framework, J. Comput. Phys. 213 (1) (2006) 141–173.
[8] R. Glowinski, T.W. Pan, T.I. Hesla, D.D. Joseph, J. Periaux, A fictitious domain approach to the direct numerical simulation of incompressible viscous flow past moving rigid bodies: Application to particulate flow, J. Comput. Phys. 169 (2001) 363–426.
[9] J. Hyman, J. Morel, M. Shashkov, S. Steinberg, Mimetic finite difference methods for diffusion equations, Comput. Geosci. 6 (2002) 333–352.
[10] K. Lipnikov, M. Shashkov, D. Svyatskiy, The mimetic finite difference discretization of diffusion problem on unstructured polyhedral meshes, J. Comput. Phys. 211 (2006) 473–491.
[11] W.J. Rider, D.B. Kothe, Reconstructing volume tracking, J. Comput. Phys. 141 (1998) 112–152.